JOC The Journal of Organic Chemistry

Article

pubs.acs.org/joc

Photochemical Oxidation of Thioketones by Singlet Molecular Oxygen Revisited: Insights into Photoproducts, Kinetics, and Reaction Mechanism

Antonio J. Sánchez-Arroyo, Zulay D. Pardo, Florencio Moreno-Jiménez, Antonio Herrera, Nazario Martín,* and David García-Fresnadillo*

Complutense University of Madrid, Department of Organic Chemistry, Faculty of Chemical Sciences, E-28040, Madrid, Spain

Supporting Information

ABSTRACT: Photosensitized oxidation of trimethyl[2.2.1]-bicycloheptane thioketones by $^1O_2$ can yield more photoproducts than exclusively ketones and sulfines. Moreover, the ketone/sulfine ratio can be reversed when protic conditions and high thioketone concentrations are used, conversely to earlier results reporting ketones as the main photoproducts. A new mechanistic proposal for sulfine formation is suggested following intermolecular oxygen transfer from a peroxythiocarbonyl intermediate to a second thioketone molecule. Reaction quantum yields (10^{-5}–10^{-2}) depend on the reaction conditions and time. Sulfine production reaches a maximum at short irradiation times, whereas decomposition to the corresponding ketone is observed at long reaction times. When the thioketone substrate has a hydrogen atom at the α position a peroxyvinylsulfenic acid intermediate can be formed by proton transfer. Reaction of this intermediate with another thioketone molecule can yield more sulfine and its tautomeric vinylsulfenic acid, which dimerizes *in situ* to the thiosulfinate. The hydroperoxyl group of the peroxyvinylsulfenic acid can also rearrange to the α position, and by reaction with the starting thioketone, α-hydroxy thioketone and additional sulfine can be formed, while dehydration yields the α-oxo thioketone. *In situ* [2 + 2] and [4 + 2] self-cycloaddition of the α-oxo thioketone yields significant amounts of the corresponding adducts at prolonged irradiation times.

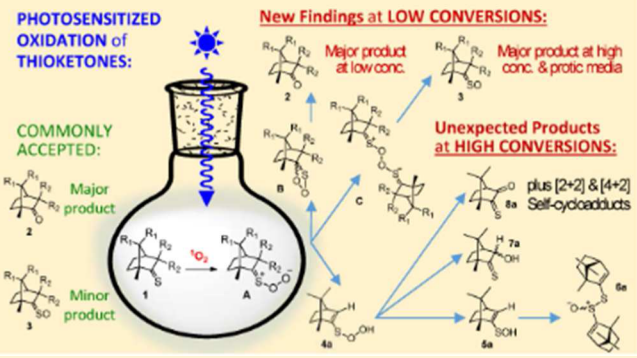

INTRODUCTION

Photosensitized and self-photosensitized oxidation of thioketones in solution and in the solid phase was mainly studied by Ramamurthy and co-workers in the 1980s, in order to develop clean oxidation methods and to reveal the mechanism of thiocarbonyls transformation into other functional groups of interest in organic synthesis.[1−7] Photosensitized oxidation of thioketones **1** yielded ketones **2** and sulfines (thiocarbonyl *S*-oxides) **3** as the isolated photoproducts, and the proposed reaction mechanism (Scheme 1) involved intramolecular SO and atomic oxygen release for ketone and sulfine formation, respectively. The ketone/sulfine ratio was governed by stereoelectronic factors operating on a zwitterionic or diradical intermediate, and in general, carbonyl compounds corresponding to desulfurization were reported as the main photoproducts. However, it was recognized that several aspects of the original mechanistic proposal were yet to be substantiated and new experimental evidence was necessary to confirm the reaction mechanism, its intermediates, and, in particular, the fate of atomic oxygen apparently produced during the reaction course as a result of sulfine formation.[5] Since then, the mechanism of photosensitized oxidation of organic compounds containing sulfur is still open to debate.[8] However, the mechanism proposed by Ramamurthy has been accepted for decades and described in several reviews and photochemistry books.[9−11]

Scheme 1. Reaction Mechanism Proposed by Ramamurthy and Coworkers for the Photosensitized Oxidation of [2.2.1]Bicycloheptane Thioketones 1[5a]

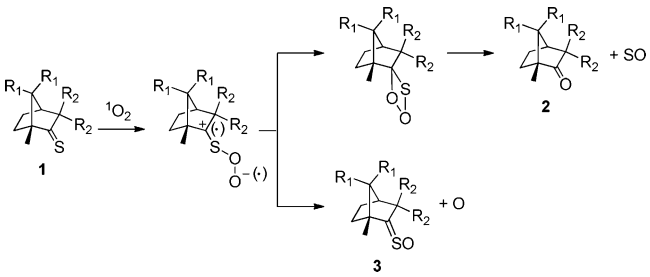

[a](1*R*)-Thiocamphor **1a**, R_1 = Me; R_2 = H. (1*R*)-Thiofenchone **1b**, R_1 = H; R_2 = Me.

Photosensitized oxidation of alicyclic thioketones **1** ((1*R*)-thiocamphor **1a** and (1*R*)-thiofenchone **1b**) was reported to

Received: July 23, 2015
Published: September 30, 2015

ACS Publications © 2015 American Chemical Society

DOI: 10.1021/acs.joc.5b01710
J. Org. Chem. 2015, 80, 10575−10584

Scheme 2. New Proposal of Reaction Scheme for the Photosensitized Oxidation of [2.2.1]Bicycloheptane Thioketones 1[a]

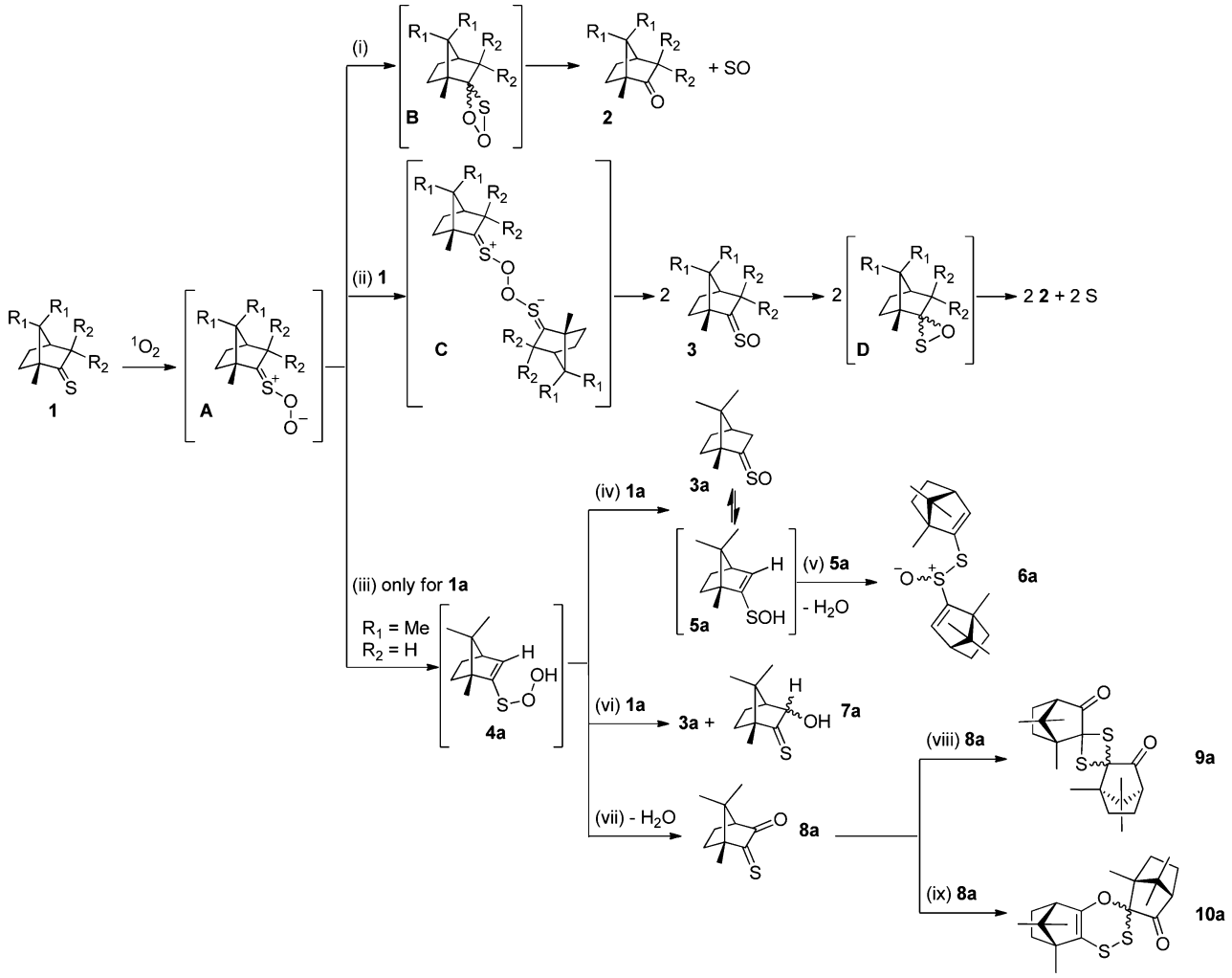

[a]New proposal of reaction pathways: (i) Low substrate concentration; ketones **2** are the major photoproducts. (ii) High substrate concentration; sulfines **3** are the major photoproducts in protic solvent or acidic conditions, while the corresponding ketones **2** are the major photoproducts in aprotic solvent. (iii) At high substrate **1a** concentration in aprotic solvent an intramolecular proton transfer from α-position to the thiocarbonyl group occurs producing the vinylpersulfenic acid **4a**. (iv) Enethiolization promoted by reaction of **1a** and **4a**. (v) Dehydration of the vinylsulfenic acid **5a** dimer to thiosulfinate **6a**. (vi) Sulfine **3a** and α-hydroxythioketone **7a** formation via intermolecular reaction of **1a** and the vinylpersulfenic acid **4a**. (vii) Dehydration of **4a** to α-oxothioketone **8a**. (viii) [2 + 2] self-cycloaddition of **8a** producing **9a**. (ix) [4 + 2] self-cycloaddition of **8a** yielding **10a**.

give, intramolecularly, the corresponding ketones **2a** and **2b** and sulfines **3a** and **3b** as the only major and minor products, respectively. However, the yield of isolated compounds for 100% conversion after >48 h irradiation was low (<50%) and attributed to difficulties in the isolation procedures and not due to any side products.[5] New oxidation experiments performed with thioketones **1a** and **1b** in the presence of photosensitized singlet oxygen allow us to give an insight into a more plausible and complete reaction mechanism (Scheme 2 and Schemes S1−S5, SI) which clarifies Ramamurthy's proposal and accounts for the formation of novel reaction products, not previously described in the literature. Moreover, we also report on the experimental conditions that can be used to photochemically promote formation of thiocarbonyl *S*-oxides as the major reaction products, instead of the corresponding ketones.

It is worth mentioning that sulfines are a unique class of sulfur-centered heterocumulenes with *Z*/*E* isomerism constituting valuable synthetic intermediates in organic chemistry, due to the variety of reactions in which they can take part (e.g., different types of cycloadditions, as reaction substrates of thiophilic and carbophilic reagents, in α-carbanion formation via tautomerization to vinylsulfenic acids, etc.).[12−14] For instance, the stereospecific [4 + 2] cycloaddition of thiocarbonyl *S*-oxides with 1,3-butadienes, where the geometry of the sulfine is retained in the cycloadduct, might be a shorter alternative route for the preparation of new dihydrothiopyran *S*-oxides and related heterocyclic compounds such as Aprikalim, a potassium channel activator with antihypertensive and antianginal activity, or derivatives thereof.[15−19]

■ RESULTS AND DISCUSSION

Evidences supporting the new proposal of reaction mechanism were collected from photosensitized oxidation experiments of thioketones **1** in (deuterated) acetonitrile or methanol in the presence of $[Ru(dip)_3]Cl_2$ dye (Φ_Δ = 0.97 ± 0.08 in methanol,[20] 0.75 ± 0.06 in acetonitrile) irradiated with a blue LED lamp (Figure S1, SI). The reaction crudes were analyzed

DOI: 10.1021/acs.joc.5b01710
J. Org. Chem. 2015, 80, 10575−10584

by a UV−vis technique at low substrate **1** concentrations (ca. 0.07 mM) or NMR and GC-MS spectrometry when irradiations were carried out at high thioketone **1** concentrations (1−80 mM).

The zwitterionic peroxythiocarbonyl intermediate **A** in Scheme 2 has been proposed to be the first formed reaction intermediate,[5] similarly to persulfoxide in reactions of singlet oxygen with organic sulfides. Persulfoxide can be described as a resonance hybrid of zwitterionic and diradical structures, although previous experimental and theoretical results are consistent with dominance of the zwitterionic form.[21] This key intermediate in the photooxidation of sulfides is a weakly bound species with a sufficient lifetime to undergo different inter- and intramolecular reactions (e.g., nucleophile/base at oxygen but also showing a trend to interconvert to intermediates often behaving as electrophilic oxidizing agents).[22] Therefore, by analogy with persulfoxide, the peroxythiocarbonyl intermediate **A** can reasonably be expected to play a significant role in the photooxidation of thioketones. Experimental evidence in favor of the parallel pathways (i) intramolecular and (ii) intermolecular in Scheme 2, arising from **A**, and their different prevalence depending on the reaction conditions, includes the following:

1. Evidence from UV−vis Spectrophotometry Experiments. UV spectral changes showed a decrease of the absorption band of thioketones **1** in acetonitrile or methanol with the irradiation time (Figures 1 and S2, SI). Reactions in acetonitrile proceeded faster. A new absorption band was observed only in methanol which matched the UV absorption peak of the corresponding thioketone *S*-oxides obtained by thermal synthesis (Table S1, Figure S3, SI). Isosbestic points (272 and 268 nm in acetonitrile and methanol, respectively) were observed except for the photooxidation of **1b** in acetonitrile, due to the expected low yield of sulfine **3b**, according to previous reports.[5] Kinetic analysis of the photosensitized oxidation in methanol at low substrate concentration (ca. 0.07 mM), where sulfine formation is small though relevant, was possible using the UV−vis spectral features of compounds **1**, **2**, and **3** (Table S1, SI). It has to be noted that, under continuous irradiation and assuming negligible quenching of the excited sensitizer by thioketones **1**, the quantum yield and the rate of **1** disappearance should be first order with respect to [**1**].[23] In agreement with the previous statement, and assuming that formation of the zwitterionic peroxythiocarbonyl intermediate **A** is the rate-determining step of the reaction, the experimental data points for the photooxidation of **1** in methanol could be fitted to first order kinetics with respect to [**1**] (Table 1, Figure 1 inset and Figure S4, SI). The asymptotic behavior at long irradiation times reveals that quasi-quantitative phototransformation of the thioketones (>96%) had been achieved, and yields of sulfines **3a** and **3b** were (24.0 ± 0.9)% and (11.0 ± 0.3)%, respectively. The quality of these results is also supported by the fraction of conversion (f) of **1** into **3**, which can be determined from the ratio of absorption coefficients of the substrate and the product at the isosbestic point wavelength ($f = \varepsilon_1^{\lambda IP}/\varepsilon_3^{\lambda IP}$, Figure S5, SI).[24] The f values in methanol for the photooxidation of **1a** into **3a** and **1b** into **3b** allowed an estimation of the yields of sulfine (28 ± 4)% and (14 ± 2)%, respectively, in good agreement with the yields of **3a** and **3b** determined from the kinetic analysis. A similar calculation for the photooxidation of **1a** into **3a** in acetonitrile gave ca. 15% of **3a** for 93% conversion of **1a** (Table 1 and Figure S2a).

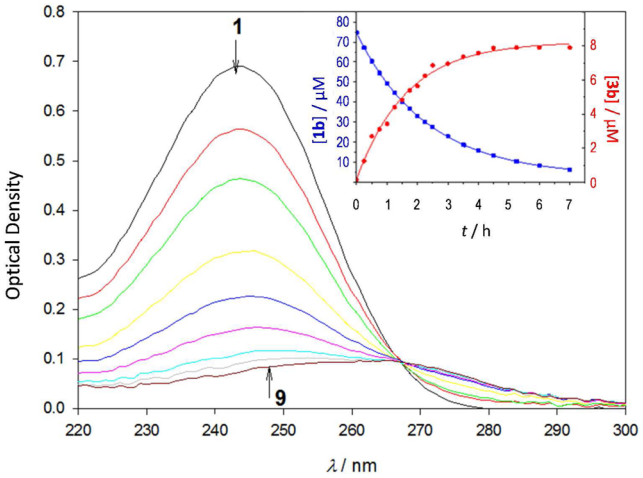

Figure 1. UV−vis monitorization of the photosensitized oxidation of **1b** in methanol at different reaction times (1:0 min, 2:30 min, 3:1 h, 4:2 h, 5:3 h, 6:4 h, 7:5 h, 8:6 h, 9:7 h). Inset: Kinetics of thioketone **1b** disappearance (blue) and sulfine **3b** formation (red).

On the other hand, the occurrence of an isosbestic point is compatible with conversion of the reaction substrate in different products via parallel reactions.[25] Therefore, the presence of the isosbestic point and the first order kinetics observed would support a reaction mechanism where parallel pathways allow competitive formation of **2** and **3** from the same parent precursor **A**, ruling out, under these conditions, a fast consecutive reaction causing decomposition of sulfines **3** into their corresponding ketones **2** and elemental sulfur, via the oxathiirane intermediate **D**.[14,26]

2. Evidence from ^{1}H and ^{13}C NMR Spectrometry Experiments. Results of the photosensitized oxidation of **1** in CD_3CN and CD_3OD (1 < [**1**] < 80 mM), monitored by NMR (accounting for 97−99% of the reaction mass) are collected in

Table 1. Experimental Results of the Photooxidation Process at Low Substrate Concentration in Methanol[a,b,c]

compound	conversion	yield	k/h^{-1}	R^2	$\Phi_{photooxidation}$	$\Phi_{photoproduction}$
1a	96.2%	–	0.499 ± 0.004	0.999	1.24×10^{-4}	–
3a	–	24.0%	0.47 ± 0.02	0.996	–	0.30×10^{-4}
1b	96.1%	–	0.431 ± 0.003	0.999	1.28×10^{-4}	–
3b	–	11.0%	0.61 ± 0.05	0.992	–	0.15×10^{-4}

[a] $[\mathbf{1a}]_0 = (7.07 \pm 0.02) \times 10^{-5}$ M; $[\mathbf{3a}]_{t\to\infty} = (1.72 \pm 0.04) \times 10^{-5}$ M; $[\mathbf{1b}]_0 = (7.44 \pm 0.02) \times 10^{-5}$ M; $[\mathbf{3b}]_{t\to\infty} = (8.2 \pm 0.2) \times 10^{-6}$ M. [b] $(1.6 \pm 0.2) \times 10^{-3}$ mol of photons absorbed during an irradiation time of 7.05 h. [c] In acetonitrile, with experimental data collected from **Figure S2(a)**, SI; $[\mathbf{1a}]_0 = (6.1 \pm 0.1) \times 10^{-5}$ M, $k = (0.65 \pm 0.01)$ h^{-1}, $R^2 = 0.999$. $\Phi_{photooxidation} = 2.7 \times 10^{-5}$ after 1.5 h of substrate **1a** irradiation. A 15.1% yield of **3a** was estimated for 93% conversion of **1a**.

DOI: 10.1021/acs.joc.5b01710
J. Org. Chem. 2015, 80, 10575−10584

Table 2. Experimental Results of the Photooxidation of Thioketones 1 at High Substrate Concentration in CD_3CN, CD_3CN + H^+, and CD_3OD[a]

compound	solvent	conversion	yield	$\Phi_{photooxidation}$	$\Phi_{photoproduction}$
1a	CD_3CN[b]	34%[e]	–[e]	8.5×10^{-3}	–
	$CD_3CN + H^+$[c]	35%	–	8.8×10^{-3}	–
	CD_3OD[d]	36%	–	9.9×10^{-3}	–
2a	CD_3CN[b]	–	14.6%[e]	–	3.6×10^{-3}
	$CD_3CN + H^+$[c]	–	9.0%	–	2.2×10^{-3}
	CD_3OD[d]	–	4.5%	–	1.3×10^{-3}
3a	CD_3CN[b]	–	4.6%[e]	–	1.2×10^{-3}
	$CD_3CN + H^+$[c]	–	13.6%	–	3.4×10^{-3}
	CD_3OD[d]	–	25.6%	–	7.1×10^{-3}
alkene-a1[f]	CD_3CN[b]	–	6.6%[e]	–	1.7×10^{-3}
	$CD_3CN + H^+$[c]	–	6.2%	–	1.5×10^{-3}
	CD_3OD[d]	–	2.0%	–	0.6×10^{-3}
alkene-a2[g]	CD_3CN[b]	–	6.0%[e]	–	1.5×10^{-3}
	$CD_3CN + H^+$[c]	–	6.0%	–	1.5×10^{-3}
	CD_3OD[d]	–	2.0%	–	0.6×10^{-3}
1b	CD_3CN[h]	8%	–	2.7×10^{-3}	–
	$CD_3CN + H^+$[i]	11%	–	2.8×10^{-3}	–
	CD_3OD[j]	29%	–	10.1×10^{-3}	–
2b	CD_3CN[h]	–	8.0%	–	2.7×10^{-3}
	$CD_3CN + H^+$[i]	–	3.6%	–	0.9×10^{-3}
	CD_3OD[j]	–	3.3%	–	1.1×10^{-3}
3b	CD_3CN[h]	–	0.0%	–	–
	$CD_3CN + H^+$[i]	–	7.2%	–	1.8×10^{-3}
	CD_3OD[j]	–	25.7%	–	8.9×10^{-3}

[a] 1.2×10^{-3} mol of photons absorbed in 3 h of irradiation. 0.8 mM concentration of $[Ru(dip)_3]Cl_2$ photosensitizer in all experiments. [b] $[\mathbf{1a}]_0 = 50 \times 10^{-3}$ M. [c] $[\mathbf{1a}]_0 = 50 \times 10^{-3}$ M, $[CF_3CO_2H] = 50 \times 10^{-3}$ M, in CD_3CN. [d] $[\mathbf{1a}]_0 = 55 \times 10^{-3}$ M. [e] After 5 h of **1a** irradiation in CD_3CN, 59% conversion of **1a** was achieved, yielding 32% of **2a**, 7.0% of **3a**, 5.2% of **alkene-a1**, and 15% of **alkene-a2**. [f] **Alkene-a1**, 6.30 ppm. [g] **Alkene-a2**, 6.05 ppm. [h] $[\mathbf{1b}]_0 = 68 \times 10^{-3}$ M, 3 h of irradiation. [i] $[\mathbf{1b}]_0 = 50 \times 10^{-3}$ M, $[CF_3CO_2H] = 50 \times 10^{-3}$ M, 3 h of irradiation. [j] $[\mathbf{1b}]_0 = 70 \times 10^{-3}$ M, 4 h of irradiation.

Table 3. Influence of the Reaction Conditions on the Ketone/Sulfine (2/3) Ratio at Low Substrate Conversions; Effect of the Initial Concentration of Thioketone in CD_3OD and of the Presence of CF_3CO_2H 50 mM in CD_3CN[a]

Substrate				CD_3OD			CD_3CN	$CD_3CN + H^+$[b]
1a[c]	$[\mathbf{1a}]_0$/mM	1	10	25	50	80	50	50
	2a/3a[d]	3.20	0.45	0.26	0.28	0.24	3.20	0.71
1b[e]	$[\mathbf{1b}]_0$/mM	1	10	40	70	80	68	50
	2b/3b[d]	0.50	0.24	0.14	0.11	0.12	–[f]	0.50

[a] Data from ^1H NMR experiments. 0.8 mM concentration of $[Ru(dip)_3]Cl_2$ photosensitizer in all experiments. [b] $[CF_3CO_2H] = 50$ mM in CD_3CN. [c] 3 h irradiation. [d] Uncertainty of **2/3**: ±10%. [e] 4 h irradiation. [f] Only ketone **2b** was detected.

Tables 2, 3 and Figures S6–S26, SI. Ketones **2** and sulfines **3** were the main reaction products but not the only ones, since new alkene-type, carbonyl and thiocarbonyl derivatives were also detected in the case of substrate **1a** (Tables 2, 3 as well as Figures S11–S14, S24–S26 and Table S3, SI). Moreover, depending on the reaction conditions (i.e., reaction time, solvent used, concentration of substrate or presence of H^+) the ketone to sulfine ratio **2/3** could be reversed (Figure 2 and Table 3). These experimental findings are in contrast to previous works claiming only one type of major product (ketone) regardless of the changes in the reaction conditions (initial concentration of substrate or aprotic/protic nature of the solvent), since only a slight dependency of the product distribution on the aprotic/protic character of the solvent was observed in previous reports.[4,5]

It has to be mentioned that, despite the longer lifetimes expected for $^*[Ru(dip)_3]^{2+}$ and, especially, $^1O_2$ in deuterated solvents, increased quenching (mainly physical, Table S2, SI) of the excited states at the high substrate concentrations used in the NMR experiments slowed down the kinetics of the photooxidation process considerably (e.g., at $[\mathbf{1a}]_0$ 50×10^{-3} M, k (0.26 ± 0.01) h^{-1} in CD_3CN; while at $[\mathbf{1a}]_0$ 6.1×10^{-5} M, k (0.65 ± 0.01) h^{-1} in CH_3CN, Table 1). Therefore, NMR monitorization was typically maintained at 3–5 h of irradiation or performed when the thioketone substrate was quantitatively depleted, as confirmed by GC-MS.

Evolution of the diagnostic signals of each compound, i.e. methyls and methylene protons in α-position to the functional group (Figures S6–11a, SI), allowed the determination of the **2/3** ratio by ^1H NMR under different reaction conditions (Table 3). Conversely to previous results, the product distribution was found to be strongly dependent on the solvent used, since the thioketone *S*-oxide can be the major product at low substrate conversions and the amount of sulfine is always higher in CD_3OD than in CD_3CN (Figure 2, Tables 2, 3, and Figures S6–S8 and S11a, SI). For example, photooxidation of thiofenchone **1b** in CD_3CN gave fenchone **2b** as the only product, with no evidence of sulfine **3b** formation, in agreement

DOI: 10.1021/acs.joc.5b01710
J. Org. Chem. 2015, 80, 10575–10584

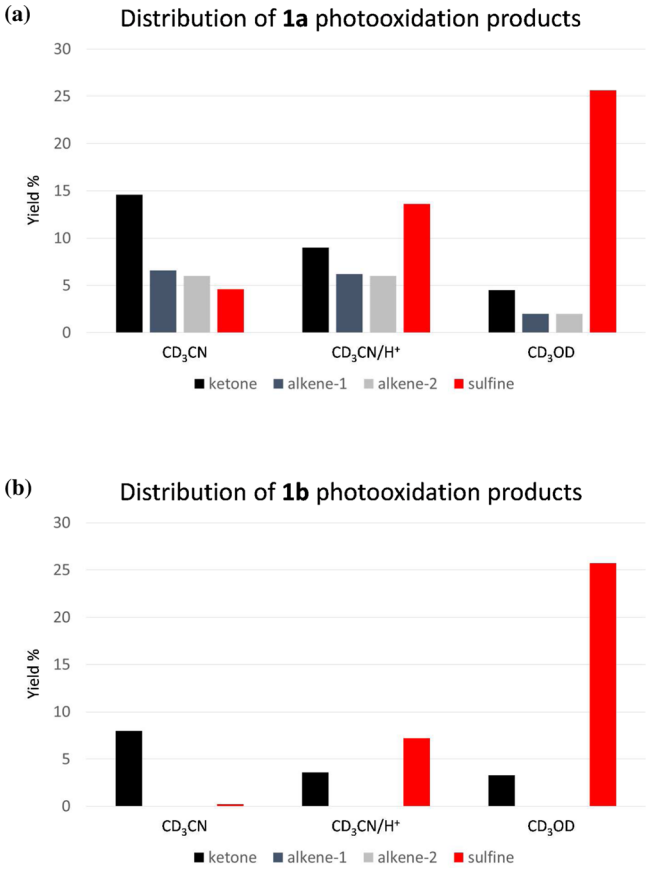

Figure 2. Distribution of the photooxidation products of thioketones **1** under different reaction conditions. Data from ^{1}H NMR experiments. (a) **1a** photooxidation; (b) **1b** photooxidation. Conversions and product yields (%) are collected in Table 2.

with UV−vis results (Figure 2 and Figures S2c and S6, SI). However, when a similar experiment was carried out in CD_3OD sulfine **3b** was the major product with an overall ratio **3b**/**2b** = 7.1 (Figure 2 and Figure S7, SI), in contrast with UV−vis results at low substrate concentration where **3b** was a minor product (Table 1 and Figure S2d, SI).

These observations would agree with the existence of an intermolecular reaction pathway for sulfine formation and also with the stabilization of the zwitterionic peroxythiocarbonyl intermediate **A** by hydrogen (deuterium) bonding with methanol molecules (Schemes S1a and S1b, SI), as proposed by Ramamurthy.[5] Therefore, in protic solvents such as methanol, intramolecular ring closure to **2** by pathway (i) via the highly unstable 1,2,3-dioxathietane intermediate **B** would be retarded, while production of **3** at sufficient substrate concentration would be favored by the intermolecular pathway (ii), through the intermediate **C**. As a result, sulfines could be major reaction products in protic solvents at short reaction times, in contrast to general assumptions (Figure 2). Similarly to the role played by *m*-chloroperbenzoic acid in thermal oxidations of thioketones, or by persulfoxide species in the photooxidation of organic sulfides, the zwitterionic peroxythiocarbonyl intermediate **A** would also behave as an oxygen atom donor to another thiocarbonyl molecule in its surroundings.

Concerning thiocamphor **1a** photooxidation, the ^{1}H NMR spectra in CD_3CN (Figure S11, SI) evidenced formation of ketone **2a** as the major product and, surprisingly, sulfine **3a** was also detected, in contrast with **1b** photooxidation in the same solvent, where sulfine **3b** product was not present. On the other hand, besides **2a** and **3a** formation, other unknown compounds (Figure 3 and Figures S8, S11−S13, SI) showing doublet signals evolving in the alkene region between 6.00 and 7.00 ppm (Tables 2 and S3, SI) were detected in CD_3CN and, to a minor extent, in CD_3OD as well. It has to be noted that no signals in the alkene region were detected when thiofenchone **1b** was photooxidized (Figure S6, SI). The observed coupling

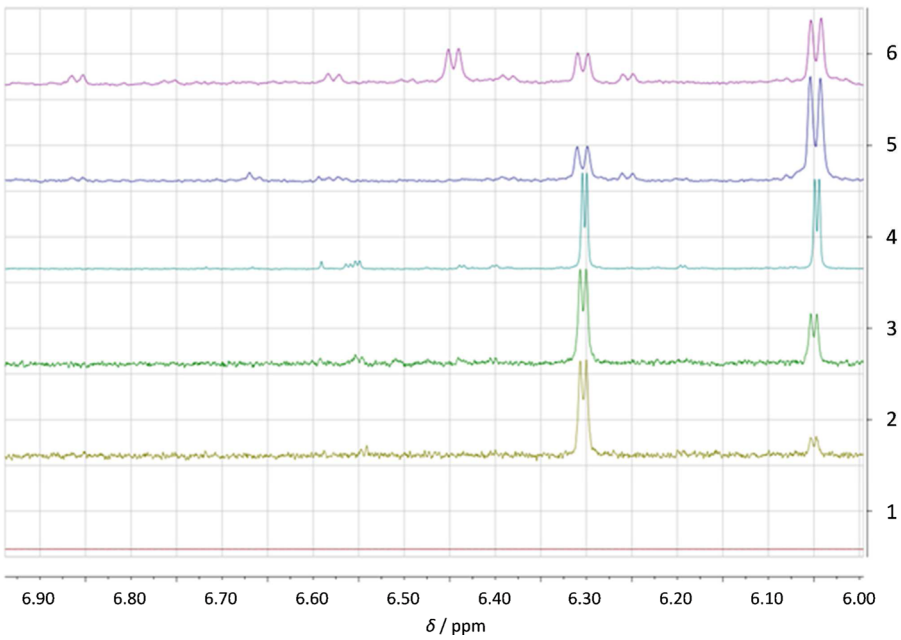

Figure 3. Evolution of the ^{1}H NMR signals in the alkene region by irradiation of **1a** in CD_3CN for 22 h. ^{1}H NMR spectra (500 MHz) collected at 0 h, red (spectrum 1); 1 h, olive (spectrum 2); 2 h, green (spectrum 3); 3 h, cyan (spectrum 4); 5 h, blue (spectrum 5); 22 h, purple (spectrum 6, 300 MHz). $[\mathbf{1a}]_0 = 50 \times 10^{-3}$ M.

DOI: 10.1021/acs.joc.5b01710
J. Org. Chem. 2015, 80, 10575−10584

constant for the alkene signals detected in **1a** photooxidation was always 3.3 Hz, corresponding to coupling of alkenic and bridgehead protons, as demonstrated by COSY correlations (Figure S12, SI) and also by experimental data from other structurally related compounds (Experimental section). A signal at 6.30 ppm appeared at shorter irradiation times, while a doublet at 6.05 ppm showed up at longer times (>1.5 h). Surprisingly, the signal at 6.05 ppm increased at the expense of that at 6.30 ppm and a new doublet at 6.45 ppm was detected after 22 h of irradiation, when **1a** was quantitatively depleted. This new signal grew at the expense of that at 6.05 ppm (Figure 3), and other additional signals were also detected after 22 h of irradiation (Figure S1, SI).

Formation of alkene derivatives from substrate **1a** could be explained by the tendency of the terminal oxygen in the zwitterionic peroxythiocarbonyl intermediate **A** to stabilize its negative charge via intramolecular proton transfer when there are hydrogen atoms available in the α-position to the thiocarbonyl group attacked by singlet oxygen (Scheme S2, SI). By analogy with the Schenck-ene reaction (Scheme S6, SI) and also in agreement with the typical reactivity of persulfoxide intermediates (removal of a α-hydrogen leading to hydroperoxysulfonium ylide formation),[8,27,28] proton transfer in the zwitterionic peroxythiocarbonyl intermediate **A** and double bond migration would lead to production of a vinylpersulfenic acid derivative **4a**. Formation of **4a** would be promoted in acetonitrile but minimized in methanol due to stabilization of **A** by the protic solvent (Figure 3 and Scheme S1, SI). Chemical evolution of **4a** via intermolecular reactions could explain the development of additional ^{1}H NMR signals in the alkene region (Schemes 2 and S2, S4, SI).

It is noteworthy that the broad singlet signal corresponding to residual water was slightly deshielded from 2.2 to 2.3 ppm during the reaction course (Figure S14, SI). It must also be noted that when photooxidation experiments of thioketones **1** were carried out in the presence of DABCO (1,4-diazabicyclo-[2.2.2]octane), a well-known singlet oxygen quencher,[29] the formation of products was slowed down and, in the case of **1a** in CD_3CN, alkene signals were completely suppressed (Figures S15 and S16, SI), demonstrating that the evolution of alkene byproducts is linked to singlet oxygen production in the reaction system.

It has been previously reported that protic conditions in photooxidation reactions of sulfur compounds can stabilize reaction intermediates bearing electrostatic charge,[30] and this effect could be of major importance in those cases where different products can be formed from the same reaction intermediate, since its stabilization can modify the ratio between products. In this sense, and taking into account that the **2**/**3** ratio is higher in CD_3OD than in CD_3CN, the addition of protons to an aprotic solvent such as CD_3CN could help to reverse the sulfine/ketone ratio in favor of the thioketone *S*-oxide product. Addition of an equimolar amount of trifluoroacetic acid to a 50 mM solution of thioketones **1** in CD_3CN, and subsequent irradiation, evidenced improved production of the corresponding sulfines **3** (Table 3, Figure 2, and Figures S17 and S18, SI). A control experiment carried out for 3 h in the dark showed no evolution of the reaction substrates by ^{1}H NMR. Moreover, formation of alkenes was also significant when trifluoracetic acid was added to **1a** in CD_3CN. Therefore, the intermolecular pathway leading to sulfine **3a** is prevalent at high substrate **1a** concentrations in protic solvents such as methanol and in acidic conditions as well (Table 3 and Figure 2).

Considering the previous results, a study on the influence of the initial concentration of substrates **1** on the products distribution was undertaken in CD_3OD. Experimental results are collected in Table 3. The intense singlet signals of products **2** and **3** near 1.0 ppm, corresponding to the methyl groups of the ketones and thiocarbonyl *S*-oxides, were used to determine the relative ratios of the photoproducts (Figures S19 and S20). The results of ^{1}H NMR experiments after 3−4 h of photosensitized irradiation in CD_3OD showed that the **2**/**3** ratio decreases as the initial concentration of substrate **1** increases, again suggesting that an intermolecular reaction pathway is involved in sulfine formation.

It has to be noted that as the reaction time of **1a** photooxidation in CD_3CN increases, the **2a**/**3a** ratio also tends to increase (e.g., **2a**/**3a** = 3.0 after 3 h, while **2a**/**3a** = 4.6 after 5 h of irradiation, and whereas **2a** was the major reaction product after 22 h of irradiation, **3a** signals were undetectable by ^{1}H NMR; Table 2 and S3, SI). Significant decomposition of sulfine **3a** at room temperature and in the dark was confirmed after 2 days in CD_3CN solution (Figure S21, SI). Therefore, slow decomposition of **3a** could occur in the reaction crude at long reaction times or, alternatively, by its participation in subsequent secondary reactions.

^{13}C NMR spectra of the reaction crudes at long irradiation times evidenced the presence of new signals of little intensity in the alkene region (Figure S22, SI) in agreement with results from ^{1}H NMR, but also in the carbonyl region at 211.1 and 212.6 ppm (Figure S23, SI), and thiocarbonyl region 277.0 ppm (Figure S24, SI), that could be attributed to new keto and thioketo species formed during the thermal evolution of the reaction crude.

3. Evidence from GC-MS Spectrometry Experiments. GC-MS spectrometry was used to analyze the reaction crude of photooxidized **1a** in CD_3CN, in the search for the new byproducts (Figures S25−S41, SI) formed by dark reactions occurring simultaneously with the photooxidation process but whose structure could not be elucidated by NMR. After continuous irradiation for 22 h, thiocamphor **1a** was quantitatively depleted (undetectable by NMR) but gave a residual peak (m/z: exp. 168.1, Figure S27, SI) by GC-MS. Camphor **2a** (m/z: exp. 152.1, Figure S26, SI) was found by both ^{1}H NMR and GC-MS (major peak of the chromatogram, Figure S25a, SI). On the other hand, no signals of thiocamphor *S*-oxide **3a** were found by ^{1}H NMR, but a GC-MS peak (m/z: exp. 184.1, Figure S30, SI) that could be attributed to sulfine **3a** or its isomeric vinylsulfenic acid **5a** was detected. However, due to the expected thermal instability of sulfines and sulfenic acids at the high temperatures used in gas chromatography, this peak could most likely correspond to the α-hydroxy thioketone **7a**, isobaric with **3a** and **5a**, in agreement with the occurrence of a new thiocarbonyl peak observed by ^{13}C NMR (277.0 ppm, Figure S24, SI) corresponding, most likely, to the *endo* diastereoisomer. Formation of α-hydroxythiocamphor **7a** could be explained via the vinylpersulfenic acid **4a** generated by proton transfer from intermediate **A** (Scheme S2, SI), and a subsequent reaction through intermediates **I**−**L** and **M** according to the reaction pathway (vi) depicted in Scheme S3, SI. GC-MS clues supporting the formation of the vinylpersulfenic acid **4a** or its isobaric isomer **L** have been found (m/z: exp. 200.1, Figure S31; and m/z: exp. 199.9, Figure S32, SI), although these compounds are also isobaric

DOI: 10.1021/acs.joc.5b01710
J. Org. Chem. 2015, 80, 10575−10584

with the highly thermally unstable and less likely detectable 1,2,3-dioxathietane intermediate **B** (Scheme S1, SI). Evidence of a cyclic derivative of **4a** generated during the analysis by loss of molecular hydrogen at the high temperatures in the chromatograph, most likely from intermediate **I** (Scheme S3, SI), has also been detected (*m*/*z*: exp. 198.1, Figure S29, SI). Moreover, α-oxo thioketone **8a** (*m*/*z*: exp. 182.1, Figure S28, SI) has been detected as well, and its formation could be justified by the intramolecular dehydration process shown in the reaction pathway (vii) (Scheme S3, SI).

Four intense peaks related to intermolecular reactions of **8a**, which can be attributed to the different diastereoisomers of adducts **9a** and **10a** formed via the [2 + 2] and [4 + 2] self-cycloadditions of **8a**, have been detected as well (*m*/*z*: exp. 364.1, Figures S37 and S39−S41, SI). Three also intense chromatographic peaks corresponding to decomposition by-products of these adducts by loss of one (*m*/*z*: exp. 332.2, Figures S35 and S36, SI) or two sulfur atoms (*m*/*z*: exp. 300.3, Figure S33, SI) were also detected, as could be expected for the two possible byproducts related to the loss of one sulfur atom, and only one byproduct when two sulfur atoms are extruded from **10a**. The two carbonyl peaks observed by ^{13}C NMR at 211.1 and 212.6 ppm (Figure S23, SI) could therefore be assigned to the most abundant diastereoisomers of these adducts. Although several carbonyl signals could be expected from **8a**, **9a** (C_2 symmetry group) and **10a** products, since self-cycloaddition reactions of **8a** are expected to occur rapidly after **8a** formation, it is likely that the observed carbonyl peaks correspond to the most stable diastereoisomers among the four possible structures of adducts **9a** and **10a**. Fast *in situ* [2 + 2] and hetero-Diels−Alder [4 + 2] self-cycloaddition reactions of α-oxo thioketones have previously been described.[31−34]

In order to explain the different signals observed by ^{1}H NMR in the alkene region between 6 and 7 ppm, and their evolution with time, the GC-MS peaks of low intensity (*m*/*z*: exp. 200.1, Figure S31; and *m*/*z*: exp. 199.9, Figure S32, SI) would support the formation of vinylpersulfenic acid **4a** (Scheme S2, SI), since at least one if not both peaks could be tentatively assigned to **4a** and/or its **L** isomer (Scheme S3, SI). On the other hand, the enethiolization of sulfines to vinylsulfenic acids has previously been described using catalytic amounts of pyridinium *p*-toluenesulfonate,[35,36] and it is likely that reaction of **4a** with **1a** could play a similar role yielding **3a** in equilibrium with **5a** (Scheme S2, SI). In this sense, it is quite remarkable the presence of a peak corresponding to one of the two possible diastereoisomers of thiosulfinate **6a** (*m*/*z*: exp. 350.2, Figure S38, SI) formed by dimerization of **5a** and subsequent dehydration via an intermediate such as **N**, in agreement with the typical chemistry of sulfenic acids (Scheme S4, SI).[37−40] Taking into account the presence of alkene-type protons in the different reaction intermediates shown in Schemes S2 and S4 (SI), **4a**, **E−H**, **5a**, and **6a**, several signals of alkenic protons with coupling constants of 3.3 Hz could be expected in the ^{1}H NMR spectrum acquired at prolonged reaction times, in agreement with the experimental results (Figure 3 and Figure S13, SI). Further support about the occurrence of the vinylpersulfenic acid intermediate **4a** could be found in a peak (*m*/*z*: exp. 262.0, Figure S34, SI) that could be attributed to addition of inorganic sulfur to the alkene group in the cyclic derivative of **4a** generated by loss of molecular hydrogen (*m*/*z*: exp. 198.1, Figure S29, SI).[41] It has to be noted that inorganic sulfur can be produced by decomposition of sulfine **3a**; moreover, elemental sulfur can also be produced in the chromatograph by decomposition of **10a** adducts. In addition, the fragmentation pattern of the peak of *m*/*z* 262.0 includes a major peak at *m*/*z* 198.1, in good agreement with the possible formation of the proposed cyclic derivative of **4a**.

When all these experimental facts are taken into consideration, a new mechanistic proposal for the photooxidation of thioketones **1** with sensitized singlet oxygen is summarized in Scheme 2 and Schemes S1−S5. Evidence collected from UV−vis, NMR, and GC-MS experiments allows us to propose the formation of ketones **2** and sulfines **3** by intramolecular and intermolecular reaction pathways, respectively, in contrast to previous reports proposing monomolecular reactions only. Therefore, sulfine formation can now be explained without the need for intramolecular release of atomic oxygen but intermolecular oxygen transfer to another thioketone molecule from the first formed peroxythiocarbonyl zwitterionic intermediate **A**. Moreover, and also conversely to previous statements, the ketone/sulfine ratio can be reversed by controlling the reaction conditions, thus enabling the formation of thioketone *S*-oxides as the major reaction products at sufficiently high substrate **1** concentrations and relatively low substrate **1** conversions. The aprotic/protic nature of the solvent or the presence of a protic organic acid influences the stability of the first formed peroxythiocarbonyl zwitterionic intermediate **A** and, therefore, the ketone/sulfine ratio. Under aprotic conditions, intramolecular closure of the zwitterion **A** to a 1,2,3-dioxathietane intermediate **B** and a subsequent retro-[2 + 2] process yields ketone **2** plus SO fragments (intramolecular pathway (i) prevailing), as previously described by Ramamurthy. However, at sufficiently high substrate **1** concentrations and under protic or acidic conditions, the peroxythiocarbonyl intermediate **A** is stabilized or protonated to a hydroperoxythiocarbonyl intermediate **AH**$^{+}$, and the intermolecular pathway (ii) prevails. As a result, the probability of ring closure to **2** is decreased, while the chances of a bimolecular reaction with another molecule of thioketone **1** are increased, leading to production of thioketone *S*-oxide **3** as the major photoproduct (Scheme S1, SI) through solvated or protonated intermediates **C** or **CH**$^{+}$, respectively. However, and in agreement with previous reports, the studied sulfines **3** tend to slowly decompose in the dark, due to their thermal instability, giving their corresponding ketones via intermediate **D**. Therefore, efficient production of thioketone *S*-oxides **3** is limited to relatively low conversions of the reaction substrates **1**.

Of particular interest is the case where the thione bears a hydrogen atom at the α-position (e.g., thiocamphor **1a**) and its concentration is high enough, since experimental evidence of proton transfer to the peroxythiocarbonyl group have been found in an aprotic solvent such as acetonitrile (pathway (iii), Scheme S2, SI). Proton transfer in **1a** produces a vinylpersulfenic acid intermediate **4a** which, upon reaction with another thiocamphor molecule, promotes formation of **5a**, the usually not observed vinylsulfenic acid tautomer of **3a** (pathway (iv)). Evidence proving the photoinduced formation of unsaturated intermediates and products related to **4a** and **5a** and of vinylsulfenic acid **5a** dimerization and dehydration to its thiosulfinate derivative **6a** (pathway (v), Scheme S4, SI) has been found by NMR and GC-MS spectrometry. In parallel, 1,3-migration of the hydroperoxyl group in **4a** to the α-position, followed by intermolecular reaction with another **1a** molecule would yield **3a** and the α-hydroxy thioketone **7a** (pathway (vi), Scheme S3, SI). Reaction pathways (ii), (iv), and (vi) can explain the remarkable production of **3a** from **1a** in an aprotic

DOI: 10.1021/acs.joc.5b01710
J. Org. Chem. 2015, 80, 10575−10584

solvent such as acetonitrile, while production of **3b** from **1b** was not observed in the same solvent. 1,3-Migration of the hydroperoxyl group in **4a** and subsequent intramolecular dehydration account for relevant α-oxo thioketone **8a** formation (pathway (vii), Scheme S3, SI). Self-cycloaddition reaction of **8a** yields cycloadducts **9a** (pathway (viii)) and **10a** (pathway (ix)) (Scheme S5, SI), which have been detected by their moderately intense peaks in GC-MS experiments (Figures S25, S37, and S39−41, SI) and the intense peaks of the decomposition products of **10a** (Figures S33, S35, and S36, SI). All these reaction pathways, not previously reported in the literature about photosensitized oxidation of thioketones **1**, are supported by experimental facts and are coherent with our new mechanistic proposal based on the competition between intra- and intermolecular reaction pathways starting from the first formed peroxythiocarbonyl reaction intermediate **A**.

■ CONCLUSIONS

A new reaction scheme for the photosensitized oxidation of thioketones **1** with singlet molecular oxygen is proposed, which explains the product distribution and its strong dependence on the reaction conditions (substrate concentration, solvent nature, and acidic medium) and time of irradiation. In addition, our mechanistic proposal can explain, in the case of thioketones with hydrogens in α position to the thiocarbonyl group, such as thiocamphor **1a**, the formation of reaction products not previously described in the literature for the photosensitized oxidation of thiocarbonyls (vinylsulfenic acid derivatives, α-hydroxy thioketones and α-oxo thioketones, and their 1,3-dithietane and 1,3,4-oxadithiin cycloadducts).

■ EXPERIMENTAL SECTION

Reagents and Solvents. D-(+)-Camphor (+97%) and L-(−)-fenchone (+98%) were the substrates used in the preparation of the corresponding thioketones. Tris(4,7-diphenyl-1,10-phenanthroline)ruthenium(II) dichloride ($[Ru(dip)_3]Cl_2$)[20] was used as the singlet oxygen photosensitizer. DABCO (1,4-diazabicyclo-[2.2.2]octane) (97%) was used as a singlet oxygen quencher. Acetonitrile (99.85%, H_2O < 0.02%), deuterated acetonitrile (H_2O < 0.05%, 99.8% D), methanol (99.9%, H_2O < 0.02%), and deuterated methanol (d_4) (H_2O < 0.03%, 99.8% D) were used as the solvents in photooxidation experiments, and trifluoroacetic acid (≥99.5%) was used for those photooxidation experiments in acidic conditions. Lawesson's reagent (99%) and *m*-chloroperbenzoic acid (75%) were used in the preparation of D-(+)-camphor and L-(−)-fenchone thioketones and sulfines, respectively. Sulfuric acid (95−97%), 1,10-phenanthroline (≥99%), sodium acetate (99%), and potassium ferrioxalate were used in actinometry experiments to determine the photon flux absorbed by the irradiated systems where the photo-oxidation reactions were carried out. Potassium ferrioxalate was synthesized according to literature procedures.[42,43] Briefly, 1.5 M solutions of iron(III) chloride (97%), $FeCl_3$ (15 mL), and potassium oxalate monohydrate (98.8−101.0%), $K_2(C_2O_4)\cdot H_2O$ (45 mL), in distilled and deionized water were mixed in a beaker under red light (GU10 red LED lamp 230 V; λ_{em}^{max} 638.0 nm, 22 nm fwhm). A precipitate was formed after 10 min of magnetic stirring. The amorphous solid was filtered and recrystallized three times in water. Light-green crystals were obtained (33%) and stored in an amber vial.

Experimental Setup Used in the Irradiation Experiments. A LED lamp (GU10 blue LED 240 V, 1.8 W T/C; λ_{em}^{max} 463.5 nm, 22 nm fwhm, Figure S1, SI) was used to illuminate either a quartz cell (10.00 mm optical length) or a standard NMR tube placed 5 cm away from the LED lamp. Homogenization of the illuminated solutions and equilibration with air was achieved with a 3 mm × 1 mm magnetic bar and a magnetic stirrer placed below the irradiated vessels (Figure S1, SI). Air equilibration was assured during the experiments by periodically removing the caps of the quartz cell and NMR tube. Reproducibility of the illumination geometry was possible with a piece of graph paper on top of the magnetic stirrer and an appropriate holder for the NMR tube. The whole illumination system was mounted inside a rigid box equipped with a sliding cover. The interior of the illumination system was lined with pieces of black card. Temperature during the irradiation experiments was 21 ± 2 °C.

Chemical Actinometry. In order to determine the amount of photons absorbed by the specific geometries of the irradiated systems, i.e., quartz cells of 10 mm optical path length (3 mL) and standard NMR tubes (0.6 mL), the following procedure assuring total absorption of incident light was used:[42,43]

Six samples of 3 mL (V_1) each were prepared, under red light, from a 0.15 M stock solution of potassium ferrioxalate in H_2SO_4 0.05 M. Each sample was added, under red light, to a 10 mm quartz cell containing a 3 mm × 1 mm magnetic bar. The quartz cell was placed, under red light, inside the box used for the irradiation experiments and care was taken to ensure reproducibility of the relative geometry with respect to the blue LED lamp. The samples were exposed to blue light for 5, 10, 30, 60, 90, and 120 s, respectively. Conversions of Fe(III) to Fe(II) were always below 5% for all the irradiation times used. A blank sample was also prepared under red light with 0.1 mL of the aforementioned stock solution in a glass vial, which was kept in the dark. A buffered solution of 1,10-phenanthroline 0.1% (w/v) was prepared in a 25 mL volumetric flask with 0.0250 g of 1,10-phenanthroline, 3.3944 g of sodium acetate, and H_2SO_4 0.5 M. 0.1 mL (V_2) of each irradiated solution were added to a vial. One mL of distilled and deionized water and 0.5 mL of 1,10-phenanthroline buffered solution were added to the vials containing each irradiated sample and also to the vial with the blank sample, for a total volume of 1.6 mL (V_3) in each vial. These solutions were stirred and kept in the dark for 1 h to allow quantitative formation of the tris(1,10-phenanthroline)iron(II) complex. Absorbance of each solution at 510 nm was measured (triplicates) in quartz cells of 1 mm optical path length in order to determine the amount of Fe(II) formed as a result of the radiation absorbed by the illuminated system. The same procedure was used for the standard NMR tube geometry, except V_1 = 0.6 mL. Calibration graphs corresponding to each geometry are shown in Figure S42, SI.

Photooxidation Experiments and Analysis of Reaction Crudes. Photosensitized oxidation of thioketones was carried out in quartz cells (10 mm optical path length) and standard NMR tubes (5 mm outer diameter) in the presence of $[Ru(dip)_3]Cl_2$ photosensitizer (Figure S1, SI). The photooxidation process was monitored at different time intervals by UV−vis spectrophotometry, ^1H and ^{13}C NMR spectrometry (300, 500, and 700 MHz for ^1H, and 75, 125, and 176 MHz for ^{13}C, respectively; spectra were referenced to residual solvent signals at $\delta_{H/C}$ 1.94/1.39 and 118.3 ppm (acetonitrile-d_3) or 3.31/49.15 ppm (methanol-d_4) relative to tetramethylsilane as the internal standard) or GC-MS (injection of 1 μL of the irradiated reaction crude on a GC system coupled to a mass selective detector under the following conditions: column (5% phenylmethylsiloxane) 30 m × 0.25 mm × 0.25 μm; carrier gas, helium; injector temperature, 220 °C; oven temperature, 70 °C, 2.5 °C/min, 300 °C; interface temperature, 150 °C; ion source, 230 °C; electron energy, 70 eV).

The volumes of the irradiated solutions (containing thioketone substrate, photosensitizer, and the corresponding solvent) were 3 and 0.6 mL for the quartz cells and NMR tubes, respectively. In order to avoid sample dilution, UV−vis monitorization was carried out with solutions of ca. 7×10^{-4} M thioketone and ca. 5×10^{-6} M $[Ru(dip)_3]Cl_2$ photosensitizer (using quartz cells of 10.00 mm or 1.00 mm optical length). The fraction (F) of incident photons absorbed by the singlet oxygen photosensitizing dye was calculated using the equation $F = 1-10^{-A}$, where A is the absorbance of the photosensitizer in the 420−530 nm range (average value A = 0.276, i.e. ∼47% of the incident photons are absorbed by the dye in the quartz cell). On the other hand, NMR monitorization was performed with 1−80 mM thioketone **1** solutions containing $[Ru(dip)_3]Cl_2$ 0.80 mM. This concentration of photosensitizer assured total absorption of the incident photons entering the NMR tube (determined by chemical

DOI: 10.1021/acs.joc.5b01710
J. Org. Chem. 2015, 80, 10575−10584

actinometry). The 220−300 nm spectral region was chosen for UV−vis monitorization since compounds **1** and **3** show strong absorption bands with distinct peaks in the selected wavelength interval, while ketones **2** display very weak absorption ($\varepsilon \leq 30$ M^{-1} cm^{-1}) and, therefore, have a negligible spectral contribution compared to that of compounds **1** and **3**.

Analysis of the Distribution of Products and the Reaction Kinetics. Using the absorption coefficients (ε/M^{-1} cm^{-1}) of sulfines **3** in the wavelength interval from 285 to 295 nm, where the thioketone substrates **1** and the ketone photoproducts **2** present negligible absorption, the sulfine concentrations at different times during the irradiation process could be determined by UV−vis spectrophotometry for the photooxidation experiments in methanol (Figures S2−S4, SI). Similarly, taking into account the concentration of photogenerated sulfine, the concentration of the remaining thioketone could be estimated.

In ^{1}H NMR experiments, the characteristic signals of the reaction substrates **1** and products **2** and **3** in the regions of the α-methylene and methyl protons were used to determine the product distributions and their concentrations at different time intervals (Figures S6−S11 and S17−S20, SI). Examples of 1,7,7-trimethylbicyclo[2.2.1]hept-2-ene derivatives with sulfur substituents at position 2, which are structural analogues of **4a**, **5a**, or **6a** having alkenic protons showing coupling constants of ca. 3.3 Hz with their corresponding bridgehead protons, are given in Figure S43, SI, together with data from their NMR spectra.[44]

A multipeak fitting procedure using a Voight function was employed to calculate the area under the respective methyl peaks of the **1a** reaction crudes in CD_3OD (Figure S20, SI).

Synthesis of thioketones and their sulfines:

- Synthesis of (1*R*)-thiocamphor **1a** and (1*R*)-thiofenchone **1b**. Thioketones **1a** and **1b** were prepared by refluxing 13.5 mmol of the corresponding ketones D-(+)-camphor and L-(−)-fenchone, respectively, with Lawesson's reagent (6.75 mmol) in dry toluene (50 mL) under an argon atmosphere for 15 days. Monitorization of the reaction crude by gas chromatography (carrier gas: nitrogen; injector and detector temperature: 220 °C; column temperature: 100 °C; injected volume: 0.60 μL) allowed detection of the remaining ketone. Solvent removal under vacuum and subsequent column chromatography (silica gel, hexane) yielded 80% of an orange solid **1a** or liquid **1b**, respectively. Characterization of the pure products agreed with literature data.[5] Spectral data of **1a**: ^{1}H-RMN (CD_3CN, 300 MHz, Figure S44, SI) δ/ppm: 2.81 (dm, J = 21.0 Hz, 1H, CH_{exo}−CO); 2.44 (d, J = 21.0 Hz, 1H, CH_{endo}−CO); 2.22 (t, J = 4.2 Hz, 1H); 2.10−2.00 (m, 1H); 1.89−1.79 (m, 1H); 1.47−1.38 (m, 1H); 1.30−1.21 (m, 1H); 1.10 (s, 3H); 1.08 (s, 3H); 0.72 (s, 3H). ^{13}C-RMN (CD_3CN, 75 MHz) δ/ppm: 274.1; 69.6; 55.7; 49.1; 45.4; 34.2; 27.1; 19.4; 19.3; 13.0. UV−vis (CH_3CN) λ_{abs}^{max}/nm (ε/M^{-1} cm^{-1} (±7%)): 479 (12), 247 (8750), 214 (3030). UV−vis (CH_3OH) λ_{abs}^{max}/nm (ε/M^{-1} cm^{-1} (±7%)): 480 (11), 247 (9320), 214 (3960). Spectral data of **1b**: ^{1}H-RMN (CD_3CN, 300 MHz, Figure S45, SI) δ/ppm (J/Hz): 2.33 (s, 1H); 1.87 (d, J = 9.9 Hz); 1.80−1.63 (m, 4H); 1.28 (s, 3H); 1.24−1.18 (m, 1H); 1.16 (s, 3H); 1.12 (s, 3H). ^{13}C-RMN (CD_3CN, 75 MHz) δ/ppm: 280.3; 67.3; 58.7; 47.8; 44.2; 36.3; 29.0; 26.8; 25.6; 19.5. UV−vis (CH_3CN) λ_{abs}^{max}/nm (ε/M^{-1} cm^{-1} (±7%)): 477 (12), 244 (8915), 218 (sh) (4160). UV−vis (CH_3OH) λ_{abs}^{max}/nm (ε/M^{-1} cm^{-1} (±7%)): 477 (11), 244 (8640), 218 (sh) (3380).
- Thermal synthesis of the (1*R*)-thiocamphor sulfine **3a** and (1*R*)-thiofenchone sulfine **3b**.[45] The experimental procedure was carried out according to literature data. **3a** 72% yield (*E* diastereoisomer only), **3b** 46% yield (80:20, *Z*/*E* mixture of diastereoisomers). Structural characterization of **3a** and **3b** agreed with literature data.[5,45] Spectral data of **3a**: ^{1}H-RMN (CD_3CN, 300 MHz) δ/ppm: 2.95 (dm, J = 21.0 Hz, 1H, CH_{exo}−CO); 2.46 (d, J = 21.0 Hz, 1H, CH_{endo}−CO); 2.04 (t, J = 4.2 Hz, 1H); 1.92−1.82 (m, 2H); 1.54−1.39 (m, 2H); 1.10 (s, 3H); 0.95 (s, 3H); 0.83 (s, 3H). ^{13}C-RMN (CD_3CN, 75 MHz) δ/ppm: 210.2; 56.1; 50.1; 44.3; 38.1; 35.5; 26.9; 19.2; 18.2; 12.0. UV−vis (CH_3OH) λ_{abs}^{max}/nm (ε/M^{-1} cm^{-1} (±7%)): 269 (7750). Spectral data of **3b**: ^{1}H-RMN (CD_3CN, 300 MHz) δ/ppm: *Z* diastereoisomer methyl groups: 1.54 (s, 3H); 1.51 (s, 3H); 1.37 (s, 3H) and *E* diastereoisomer methyl groups: 1.80 (s, 3H); 1.36 (s, 3H); 1.35 (s, 3H). ^{13}C-RMN and DEPT-135 (CD_3CN, 75 MHz) δ/ppm: *Z* diastereoisomer: 218.0 (C, C═S═O); 55.4 (C); 52.8 (C); 50.1 (CH); 45.3 (CH_2); 38.0 (CH_2); 26.0 (CH_2); 24.2 (CH_3); 23.0 (CH_3); 18.1 (CH_3) and *E* diastereoisomer: 215.1 (C, C═S═O); 60.9 (C); 50.3 (CH); 49.7 (C); 46.5 (CH_2); 37.0 (CH_2); 31.2 (CH_3); 27.8 (CH_3); 25.5 (CH_2); 19.2 (CH_3). HMQC and HMBC spectra confirmed the signals of the *Z* and *E* diastereoisomers (Figure S46, SI). 4:1 mixture of *Z*/*E* diastereoisomers, in agreement with literature data.[45] UV−vis (CH_3OH) λ_{abs}^{max}/nm (ε/M^{-1} cm^{-1} (±7%)): 270 (7800).

Photophysical Characterization of the System under Study. The experimental setup used for the photophysical characterization has been described elsewhere.[46] Emission decay traces (10 shots/sample, λ_{exc} = 532 nm, λ_{em} = 620 nm for the photosensitizer and λ_{em} = 1270 nm for singlet oxygen) were analyzed using the Marquardt algorithm for decay analysis included in the software package of the instrument. The singlet oxygen production quantum yield of the $[Ru(dip)_3]Cl_2$ photosensitizer in acetonitrile was determined relative to Rose Bengal in acetonitrile, which was used as the reference photosensitizer (Φ_Δ = 0.71).[47] The singlet oxygen luminescence decay curves at 1270 nm following pulse laser excitation were recorded at different laser powers in the 1−10 mW range. Experimental runs at different incident powers were carried out by measuring the singlet oxygen emission decay from the solution of reference photosensitizer (Rose Bengal) initially and, consecutively, from the $[Ru(dip)_3]Cl_2$ photosensitizer. The relative ratio of the slopes of the linear plots of singlet oxygen luminescence vs the excitation laser radiant power was used to determine the singlet oxygen production quantum yield (Figure S47, SI).[23] The luminescence intensities at 1270 nm were measured using quartz cells under identical experimental conditions from identical laser pulses, and from solutions with matched absorbance at 532 nm (absorbance = 0.100 ± 0.009 at 532 nm). Stern−Volmer analysis of the emission lifetimes allowed the determination of the bimolecular deactivation rate constants collected in Table S2, SI.

■ ASSOCIATED CONTENT

Supporting Information

The Supporting Information is available free of charge on the ACS Publications website at DOI: 10.1021/acs.joc.5b01710.

Schemes of reaction depicting the proposed reaction mechanism. Experimental setup used in the photooxidation experiments. UV−vis spectra and analysis of the information retrieved from the spectral data. ^{1}H and ^{13}C 1D and 2D NMR spectra and analysis of the information retrieved from the spectral data. GC-MS data. Photophysical characterization of the sensitizer excited state and singlet oxygen in the system under study (PDF)

■ AUTHOR INFORMATION

Corresponding Authors

*E-mail: nazmar@ucm.es (N.M.).
*E-mail: dgfresna@ucm.es (D.G.-F.).

Notes

The authors declare no competing financial interest.

DOI: 10.1021/acs.joc.5b01710
J. Org. Chem. 2015, 80, 10575−10584

■ ACKNOWLEDGMENTS

The work was supported by the Ministry of Science and Innovation (Project Reference CTQ2011-24652). A.J.S.-A. thanks the Complutense University for a predoctoral grant (ref. CT4/14).

■ REFERENCES

(1) Rajee, R.; Ramamurthy, V. *Tetrahedron Lett.* **1978**, *19*, 5127−5130.
(2) Jayathirtha Rao, V.; Ramamurthy, V. *Indian J. Chem., Sect. B* **1980**, *19B*, 143−145.
(3) Ramnath, N.; Ramesh, V.; Ramamurthy, V. *J. Chem. Soc., Chem. Commun.* **1981**, 112−114.
(4) Rao, V. J.; Muthuramu, K.; Ramamurthy, V. *J. Org. Chem.* **1982**, *47*, 127−131.
(5) Ramnath, N.; Ramesh, V.; Ramamurthy, V. *J. Org. Chem.* **1983**, *48*, 214−222.
(6) Arjunan, P.; Ramamurthy, V.; Venkatesan, K. *J. Org. Chem.* **1984**, *49*, 1765−1769.
(7) Rao, V. P.; Ramamurthy, V. *Tetrahedron* **1985**, *41*, 2169−2176.
(8) Clennan, E. L.; Liao, C. *Tetrahedron* **2006**, *62*, 10724−10728.
(9) Maciejewski, A.; Steer, R. P. *Chem. Rev.* **1993**, *93*, 67−98.
(10) Corsaro, A.; Pistará, V. *Tetrahedron* **1998**, *54*, 15027−15062.
(11) Gilbert, A.; Baggott, J. *Essentials of Molecular Photochemistry*; Blackwell Scientific Publications: Oxford, 1991; pp 518−520.
(12) Zwanenburg, B. *J. Sulfur Chem.* **2013**, *34*, 142−157.
(13) Ulrich, H. *Cumulenes in Click Reactions*; Wiley: Chichester, 2009; pp 13−23.
(14) Zwanenburg, B. *Recl. Trav. Chim. Pays-Bas-J. R. Neth. Chem. Soc.* **1982**, *101*, 1−27.
(15) Lucassen, A. C. B. Sulfine-based Synthesis of Four-, Five- and Six-Membered Heterocycles. Ph.D. Thesis, Radboud University Nijmegen, Netherlands, November 2003. http://repository.ubn.ru.nl/handle/2066/19352 (accessed July 1, 2015).
(16) Philipse, H. J. F. Silyl-Mediated and Oxidative Synthesis of Sulfines. Ph.D. Thesis, Radboud University Nijmegen, Neherlands, October 2003. http://repository.ubn.ru.nl/bitstream/handle/2066/19347/19347_silyanoxs.pdf?sequence=1 (accessed July 1, 2015).
(17) Damen, T. J. G. Synthesis and Reactions of α-Oxo Sulfines and 3,6-Dihydro-2*H*-thiopyran *S*-oxides. Ph.D. Thesis, Radboud University Nijmegen, Netherlands, March 2002. http://repository.ubn.ru.nl/dspace31xmlui/bitstream/handle/2066/19104/19104_syntanreo.pdf?sequence=1 (accessed July 1, 2015).
(18) Pinto, I. L.; Buckle, D. R.; Rami, H. K.; Smith, D. G. *Tetrahedron Lett.* **1992**, *33*, 7597−7600.
(19) Bastin, R.; Albadri, H.; Gaumont, A. C.; Gulea, M. *Org. Lett.* **2006**, *8*, 1033−1036.
(20) García-Fresnadillo, D.; Georgiadou, Y.; Orellana, G.; Braun, A. M.; Oliveros, E. *Helv. Chim. Acta* **1996**, *79*, 1996−1222.
(21) Jensen, F.; Greer, A.; Clennan, E. L. *J. Am. Chem. Soc.* **1998**, *120*, 4439−4449.
(22) Clennan, E. L. *Acc. Chem. Res.* **2001**, *34*, 875−884.
(23) Wilkinson, F.; Helman, W. P.; Ross, A. B. *J. Phys. Chem. Ref. Data* **1993**, *22*, 113−263. It has to be noted that <3% of $^*[Ru(dip)_3]^{2+}$ dye is quenched when [**1**] = 1 mM compared to the very efficient quenching (> 95%) by dissolved molecular oxygen in both acetonitrile and methanol (Table S2, SI). Therefore, the steady-state approximation can be applied to all the excited states involved in the photoprocess ($^*[Ru(dip)_3]^{2+}$ and $^1O_2$). The rate of **1** disappearance is first-order with respect to [**1**] when the deactivation rate constant, k_d, of $^1O_2$ by the solvent ($k_d = 1/\tau_\Delta$, where τ_Δ is the emission lifetime of singlet oxygen in the solvent) is much higher than the product k_r·[substrate] (where k_r is the overall rate constant of $^1O_2$ depletion in the presence of the substrate, either by physical quenching or chemical reaction).
(24) Berlett, B. S.; Levine, R. L.; Stadtman, E. R. *Anal. Biochem.* **2000**, *287*, 329−333.
(25) Croce, A. E. *Can. J. Chem.* **2008**, *86*, 918−924.
(26) Carlsen, L.; Holm, A.; Koch, E.; Stilkerieg, B. *Acta Chem. Scand.* **1977**, *31b*, 679−682.
(27) Prein, M.; Adam, W. *Angew. Chem., Int. Ed. Engl.* **1996**, *35*, 477−494.
(28) Clennan, E. L. *Tetrahedron* **2000**, *56*, 9151−9179.
(29) Wilkinson, F.; Helman, W. P.; Ross, A. B. *J. Phys. Chem. Ref. Data* **1995**, *24*, 663−1021.
(30) Clennan, E. L.; Greer, A. *J. Org. Chem.* **1996**, *61*, 4793−4797.
(31) Back, T. J.; Dyck, B. P.; Parvez, M. *J. Org. Chem.* **1995**, *60*, 703−710.
(32) Crossland, I. *Acta Chem. Scand.* **1977**, *31b*, 890−894.
(33) El-Essawy, F. A. G.; Yassin, S. M.; El-Sakka, I. A.; Khattab, A. F.; Sotofte, I.; Madsen, J. O.; Senning, A. *J. Org. Chem.* **1998**, *63*, 9840−9845.
(34) Hegab, M. I.; Abd El-Galil, A. A.; Abdel-Megeid, F. M. E. *Z. Naturforsch. (B)* **2002**, *57*, 922−927.
(35) Mazzanti, G.; van Helvoirt, E.; van Vliet, L. A.; Ruinaard, R.; Masiero, S.; Bonini, B. F.; Zwanenburg, B. *J. Chem. Soc., Perkin Trans. 1* **1994**, 3299−3304.
(36) Mazzanti, G.; Ruinaard, R.; van Vliet, L. A.; Zani, P.; Bonini, B. F.; Zwanenburg, B. *Tetrahedron Lett.* **1992**, *33*, 6383−6386.
(37) Block, E.; O'Connor, J. *J. Am. Chem. Soc.* **1974**, *96*, 3929−3944.
(38) Davis, F. A.; Jenkins, R. H., Jr. *J. Am. Chem. Soc.* **1980**, *102*, 7967−7969.
(39) Gupta, V.; Carroll, K. S. *Biochim. Biophys. Acta, Gen. Subj.* **2014**, *1840*, 847−875.
(40) Li, X. B.; Xu, Z. F.; Liu, L. J.; Liu, J. T. *Eur. J. Org. Chem.* **2014**, *2014*, 1182−1188.
(41) Bulman Page, P. C.; Wilkes, R. D.; Reynolds, D. Alkyl Chalcogenides: Sulfur-based Functional Groups. 2.03.2.1.7 Dialkyl Sulfides. Formation from alkenes. In *Synthesis: Carbon with One Heteroatom Attached by a Single Bond*; Ley, S. V., Vol. Ed. In *Comprehensive Organic Functional Group Transformations*; Katritzky, A. R., Meth-Cohn, O., Rees, C. W., Eds-in-chief; Pergamon: Oxford, 1995; Vol. 2, pp 137−138.
(42) Kuhn, H. J.; Braslavsky, S. E.; Schmidt, R. *Pure Appl. Chem.* **2004**, *76*, 2105−2146.
(43) Montalti, M.; Credi, A.; Prodi, L.; Gandolfi, M. T. *Handbook of Photochemistry*, 3rd ed.; CRC Press: Boca Raton, FL, 2006; Chapter 12, pp 601−616.
(44) Álvarez García, A. M. Síntesis estereoselectiva y aplicaciones de nuevos tioderivados con esqueleto norbornánico. Ph.D. Thesis, Complutense University of Madrid, Spain, September 2008. http://eprints.ucm.es/8558/ (accessed July 1, 2015).
(45) Maccagnani, G.; Innocenti, A.; Zani, P. *J. Chem. Soc., Perkin Trans. 2* **1987**, 1113−1116.
(46) Díez-Mato, E.; Cortezón-Tamarit, F. C.; Bogialli, S.; García-Fresnadillo, D.; Marazuela, M. D. *Appl. Catal., B* **2014**, *160−161*, 445−455.
(47) Ortiz, M. J.; Agarrabeitia, A. R.; Duran-Sampedro, G.; Prieto, J. B.; Lopez, T. A.; Massad, W. A.; Montejano, H. A.; Garcia, N. A.; Arbeloa, I. L. *Tetrahedron* **2012**, *68*, 1153−1162.

DOI: 10.1021/acs.joc.5b01710
J. Org. Chem. 2015, 80, 10575−10584